Ionospheric hole behind an ascending rocket observed with a dense GPS array

Tomoaki Furuya* and Kosuke Heki

Dept. Natural History Sci., Hokkaido University, N10 W8, Kita-ku, Sapporo 060-0810, Japan

An ascending liquid-fuel rocket is known to make a hole in the ionosphere, or localized electron depletion, by leaving behind large amounts of neutral molecules (e.g. water) in the exhaust plume. Such a hole was made by the January 24, 2006 launch of an H-IIA rocket from Tanegashima, Southwestern Japan, and here we report its observation with a dense array of Global Positioning System receivers as a sudden and temporary decrease of total electron content. The observed disturbances have been compared with a simple numerical model incorporating the water diffusion and chemical reactions in the ionosphere. The substantial vanishing of the ionosphere lasted more than one hour, suggesting its application as a window for ground-based radio astronomical observations at low frequencies.
Key words: GPS, ionospheric hole, rocket launch, total electron content, radio astronomy.

1. Introduction

Ionospheric Total Electron Content (TEC) is easily measured as the phase difference of the L band carrier waves at two frequencies, L1 ($\sim$1.5 GHz) and L2 ($\sim$1.2 GHz), from Global Positioning System (GPS) satellites. TEC measurements with GPS have been contributing to solar-terrestrial studies with observations of upper atmospheric phenomena, e.g. traveling ionospheric disturbances (Saito *et al.*, 2002), sudden increase of TEC by solar flares (Zhang and Xiao, 2005), decrease by solar eclipse (Afraimovich *et al.*, 2002), the aftermath of geomagnetic storms (Mitchell *et al.*, 2005), and so on.

A localized reduction of ionization by an exhaust plume of the Vanguard II missile was detected in 1959 by ionospheric sounding (Booker, 1961). Later, Mendillo *et al.* (1975) found a sudden TEC decrease after the Skylab launch by measuring the Faraday rotation of radio signals from a geostationary satellite, and suggested that the exhaust plume of the rocket chemically influenced the ionosphere. They inferred that H_2O and H_2 in the exhaust plume became molecular ions by reacting with ambient O^+ and their dissociative recombination with e^- caused electron loss, or the formation of an ionospheric "hole". Recently, numbers of active experiments of making such holes have been performed by dedicated burns of orbital maneuver systems (OMS) of spacecraft in order to study physical processes of the formation and decay of such holes (e.g. Bernhardt *et al.*, 2005).

Past observations relied on limited numbers of ground stations with special equipments including cameras to record airglows and incoherent scatter radars to profile elec-

tron densities (Mendillo *et al.*, 1987; Bernhardt *et al.*, 1998). The recent expansion of continuous GPS networks enabled the observations of growth and decay of such holes with sufficient spatial and temporal coverage. Infrasound has been often observed to accompany rocket launches (Donn *et al.*, 1968). Calais and Minster (1996), using the GPS-TEC technique, detected such acoustic perturbation of the ionosphere, a physical influence of rocket ascent on ionosphere. Here we report one of its chemical influences, formation of an ionospheric hole, observed for the first time with a dense GPS array.

2. Data Analysis

H-IIA is a Japanese launch vehicle with a liquid hydrogen fuel engine. Its eighth launch took place at 01:33 UT (10:33 in Japan Standard Time), January 24, 2006, at Tanegashima (Fig. 1) in order to put the Advanced Land Observation Satellite (ALOS) into a polar orbit at an altitude of $\sim$700 km. The Japanese dense GPS array GEONET (GPS Earth Observation Network), composed of more than 1000 continuous GPS tracking stations, records L1/L2 phases every 30 seconds, and its raw data are available on line from www.terras.gsi.go.jp. Line-of-sights connecting Satellite 3 (and 19) and receivers in the Ryukyu Islands penetrate the ionosphere near the rocket track and are likely to record the ionospheric hole by the H-IIA rocket exhaust gas (Fig. 1).

Figure 2(a) shows 24 hours of raw TEC time series observed at one of these stations (0738) with various GPS satellites. Satellites 3 and 19 show abnormal dips in TEC shortly after the launch. Figure 2(c) compares the time series of Satellite 3 with those in the same time window on the previous and following days. We modeled these curves using second order polynomials, and inferred the curve on the launch day as their average (TEC change would have followed this curve if the launch had not occurred and if the background TEC had changed similarly). The anomalous TEC change could then be isolated as the difference be-
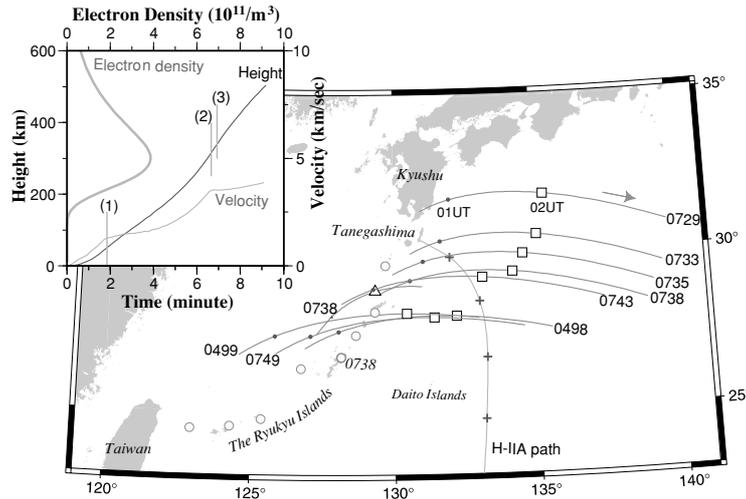
Fig. 1. Eight gray curves with time marks running parallel indicate trajectories of subionospheric points (ground projections of intersections of line-of-sights and a hypothetical surface as high as 300 km) of Satellite 3 from GPS stations in the Ryukyu Islands. The trajectories cover the period shown in Fig. 4. Numbers denote the IDs of the GPS sites (locations shown as open circles). For 0738, an additional trajectory is shown for Satellite 19 (open triangle is the 02 UT time mark). The H-IIA rocket was launched from Tanegashima, and ascended southward along the gray track (crosses show positions at altitudes 100, 200, 300, and 400 km). The height and velocity of the rocket are shown as functions of time in the inset together with the electron density profile drawn using Eq. (1) in the text. The three epochs in the inset show (1) the solid fuel booster stop (111 seconds), (2) first engine stop (399 seconds), and (3) second engine start (416 seconds).
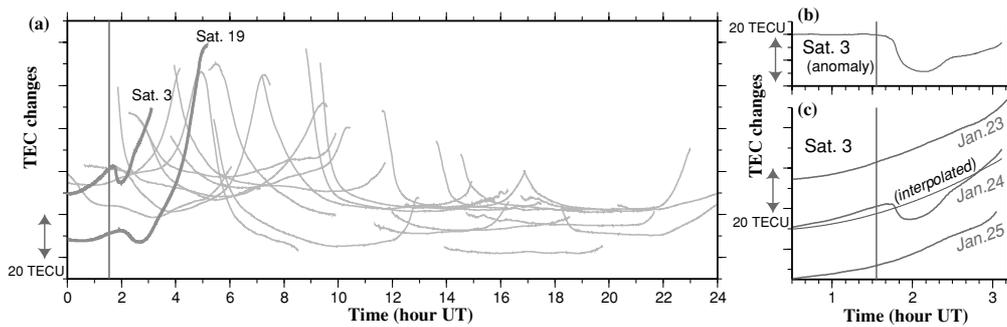

Fig. 2. (a) Raw time series of TEC on January 24 observed at 0738. Curves show TEC obtained with different GPS satellites, and their concave patterns reflect changes of satellite elevation. Satellites 3 and 19 show unusual TEC decrease shortly after the launch at 01:33 UT. In (b) we show the anomalous component of Satellite 3 TEC changes isolated as the difference from the expected curve, the average of the curves in the same period on the previous and next days (c).

tween the observed and interpolated curves (Fig. 2(b)). This procedure removes a large portion of day-to-day variability in TEC change curves due to the change in GPS satellite constellation: it gets ∼4 minutes earlier per day (Agnew and Larson, 2007).

Daily vertical TEC changes obtained by analyzing GEONET data, available on line from Kyoto University (Akinori Saito, www-step.kugi.kyoto-u.ac.jp/∼saitoua/GPS_TEC), show that the background TEC was ∼10 TEC unit (TECU, 1 TECU = 10^{16} electrons/m^2) around the time of the launch. The decreases in slant TEC exceed 10 TECU (Fig. 2(b)), and those in vertical electron content (obtained by dividing TEC by the cosine of the incident angle) reaches ∼7–8 TECU. This suggests that substantial part of the electrons were lost.

3. Model of the Ionospheric Hole Formation
3.1 Pre-launch conditions
At a point in the dayside ionosphere, electrons are continuously produced by several different processes, and we

here consider photoionization of atomic oxygen by ultraviolet and x-ray solar radiations a dominant one. The production rate (including the divergence of electron motions) f depends on the height z and the solar zenith angle θ. On the other hand, recombination of O^+ and e^-, involving intermediate reactions with N_2 and O_2, lets electrons decay naturally at a rate proportional to the electron density $n(e^-)$, i.e.

$$\frac{dn(e^-)}{dt} = -\beta_{\text{eff}} \cdot n(e^-) + f(z, \theta). \quad (1)$$

The coefficient β_{eff} is ∼ 1.98×10^{-5} at altitude 350 km (Mendillo *et al.*, 1975). The temporal changes of f result in diurnal variations of TEC. Its height dependence makes the characteristic vertical electron distribution, such as the Chapman distribution (Fig. 1 inset) expressed as

$$n(e^-) \propto \exp \frac{1 - \xi - \exp(-\xi)}{2} \qquad \xi \equiv \frac{z - h_c}{H}, \quad (2)$$

where h_c is the height of maximum ionization (∼300 km in the studied area and time; ionograms taken at one of these
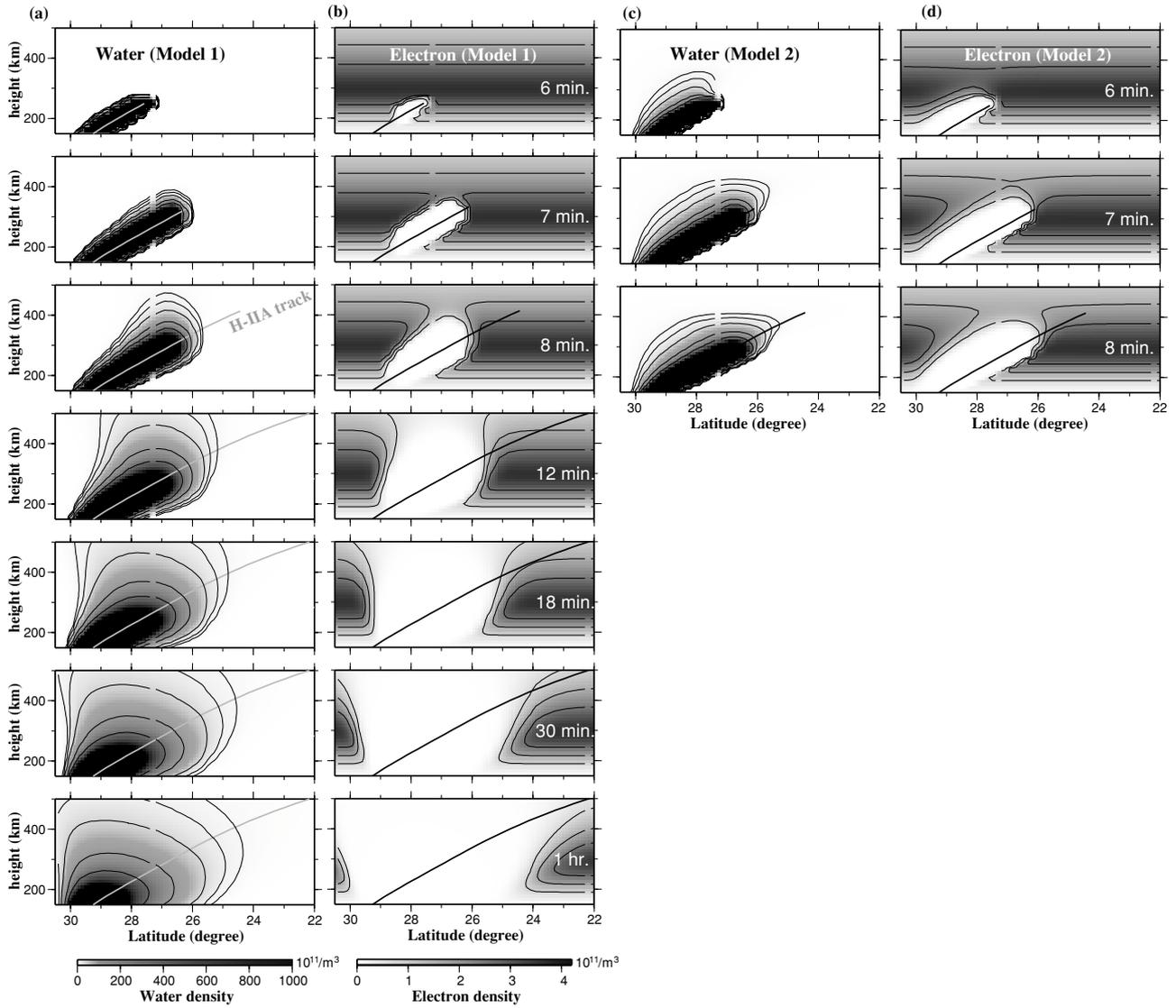
Fig. 3. The calculated densities of water molecules (a) and electrons (b) after the H-IIA launch at seven epochs (times are after the launch), shown as profiles along the H-IIA ascending track (nearly north-south). Contours show 10, 30, 50, 100, 500 × 10^{11}/m³ in (a), and 1, 2, 3 × 10^{11}/m³ in (b), respectively. The whitish region in (b) is the ionospheric hole. Anisotropic diffusion of water molecule due to height-dependent diffusivity was approximated by adopting the diffusivity at the middle point height between the source and the destination of the diffusion (Model 1). Those calculated by equations of Bernhardt (1979a) for the first three epochs are given in (c) and (d).

islands are available at wdc.nict.go.jp), and H is 65 km (Calais *et al.*, 1998). We scaled $n(e^-)$ so that the vertical TEC, $n(e^-)$ integrated over the entire z, becomes 10 TECU. Here we assume f equals $\beta_{eff} \cdot n(e^-)$, i.e. the electron density would have been stationary during the period in question if the launch had not taken place.

The exhaust plume of a rocket brings large amounts of neutral molecules (mostly H_2O from H-IIA rockets) into the ionosphere. They are highly reactive and enhance chemical recombination rates between O^+ and e^-, making an ionospheric hole. Here we model this process in two steps, i.e. diffusion of H_2O from the plume, and dissociative recombination of e^- (diffusion and reaction actually occur simultaneously). Then we calculate TEC signals expected in various GPS satellite-receiver pairs whose line-of-sight vectors penetrate the hole.

3.2 Diffusion of H_2O

Water molecules from the rocket rapidly diffuse into the atmosphere. If we neglect the initial velocity of gas (i.e. the rocket was as fast as the exhaust effusion), the molecule density at the radial distance r from a point source is

$$n(r, t) = \frac{S_0}{(4\pi D t)^{3/2}} \exp \frac{-r^2}{4Dt}, \tag{3}$$

where t is the time after the molecule release, S_0 is the total number of molecules, and D is the diffusion coefficient. Actually, gas has backward absolute velocity during the burn of the first stage engine. The specific impulse (429 second) of the rocket suggests the exhaust speed (gas speed relative to the rocket) of ~4 km/sec. Since the rocket had achieved this velocity at ~300 km height (Fig. 1 inset), the exhaust molecules should have had substantial backward velocity below that altitude. Here we neglected it because the typical travel distance of non-collisional flow,

which precedes the onset of diffusion, does not exceed a few tens of kilometers under the present situation (Bernhardt, 1979b).

We approximate continuous gas effusion from the rocket with a series of discrete point sources put along the track with a 10 second separation. The number of H_2O molecules released in unit time can be inferred from the specifications of H-IIA rockets (Osawa, 2003); the mass of the gas put into atmosphere in a second is obtained by dividing the thrust $(1.073 \times 10^6 \text{ N})$ with the specific impulse. Given the weight of an H_2O molecule, we get the number as 8.5×10^{28} every 10 seconds.

The water density $n(H_2O)$ at a certain point is the sum of n calculated by (3) from the set of point sources along the track. Equation (3) assumes isotropic diffusion, although D actually depends on altitude (i.e. larger at higher altitudes). We approximated such anisotropic diffusion with the two methods. We first used the diffusivity D at the middle point of the line connecting the rocket and the point where we calculate $n(H_2O)$ (Model 1). Secondly, we applied the approximate expression of anisotropic diffusion from a point source given in Bernhardt (1979a) (Model 2). The D at an arbitrary height is inter- or extrapolated assuming its values 2, 12 and 67 km^2/second at 250, 350, 450 km from the ground, respectively (Mendillo *et al.*, 1975). At the height of 300 km, the first stage engine was cut off, and the second stage engine started. We only considered the first engine at altitudes 100–300 km, because the thrust of the second engine is less than one tenth of the first one. Figure 3(a) shows the distribution of diffusing H_2O molecules at selected epochs by Model 1. Those by Model 2 are shown in Fig. 3(c), which suggests faster upward expansion in early periods.

3.3 Formation of the hole and penetration of line-of-sights

Artificially added water molecules react with O^+ and become H_2O^+, whose dissociative recombination with e^- causes electron depletion. By adding this loss term to Eq. (1), $n(e^-)$ after the launch changes as

$$\frac{dn(e^-)}{dt} = -\beta_{\text{eff}} \cdot n(e^-) + f(z,\theta) - \beta_{H_2O} \cdot n(e^-). \quad (4)$$

Here we assume that β_{H_2O} is proportional to the water density, i.e. $\beta_{H_2O} = 2.2 \times 10^{-15} \times n(H_2O)$, as suggested in Mendillo *et al.* (1975).

In order to model the electron density, we set up a three dimensional grid over the rectangular area 1500 km $\times$ 1500 km covering the H-IIA trajectory, and 150–700 km in altitude, with 30 km horizontal and 10 km vertical separations. We let the electron densities at the grid points evolve with time following Eq. (4) with a time step of 15 seconds in response to the changing $n(H_2O)$ and $n(e^-)$. The electron density profiles at selected epochs show rapid expansion of the hole (Fig. 3(b, d)).

In order to simulate TEC variations, we repeated the following steps every 30 seconds for each of the eight GPS stations. We first calculated the position of Satellite 3 in the Earth fixed frame using broadcast orbit, and secondly calculated $n(e^-)$ along the line-of-sight at altitudes 150–700 km in 10 km steps by interpolating from grid point
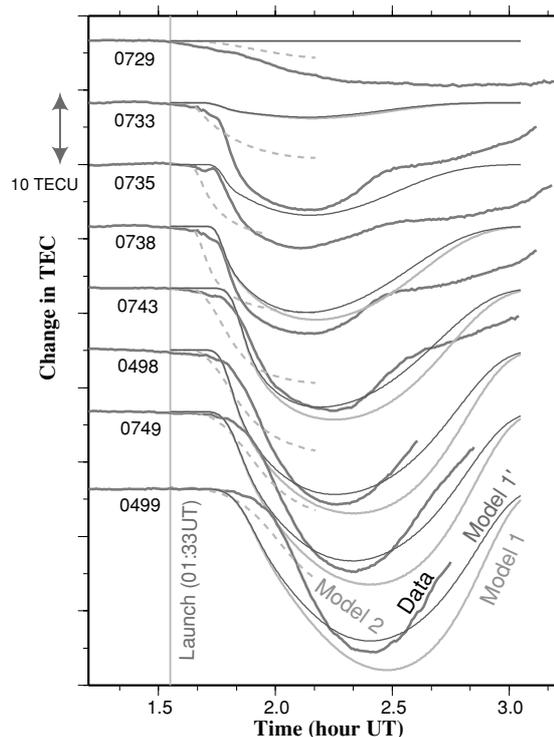

Fig. 4. Dark gray curves show anomalous changes in TEC at eight GPS stations (Fig. 1) over two hours period including the launch time. Light gray curves show TEC changes simulated by two different models for the anisotropic water diffusion (Models 1 and 2). In Model 1′ curves, natural decay of the hole with a time constant of 1.5 hour was added to those by Model 1.

values, and finally the values are integrated to obtain slant TEC at the epoch.

Figure 4 shows simulated TEC anomalies based on the two water diffusion models, i.e. the differences between the synthesized TEC and those under the normal electron distribution (Fig. 1 inset), together with the observed TEC anomalies inferred as in Fig. 2(b, c). Only the first ten minutes are shown for Model 2 considering the validity of the equation as suggested in Bernhardt (1979a). Model 2 seems to give better fits to observations in this period. The TEC recoveries after experiencing minima mainly reflect the departure of line-of-sight vectors from the hole due to the GPS satellite movement (and partly the decay of the hole). In spite of the simplicity of the models, overall agreements of the observed changes with the simulations are notable.

4. Discussion and Conclusion

In Fig. 4, southern stations suffer from the longer lasting simulated TEC anomalies. The present model neglects several factors, which might be responsible for these discrepancies. One such factor is the negligence of the second engine contribution. Its inclusion, however, degrades the fit of the southern stations and does not solve the problem. Natural photoionization contributes to the hole decay (i.e. ionosphere recovery) in Eq. (4). An improved approximation, e.g. by introducing the height dependence of β_{eff}, does not solve this problem, since β_{eff} is smaller than β_{H_2O} by several orders of magnitudes.

In Fig. 4, the curves indicated as Model 1′ were derived by adding a natural decay term of the hole with a time constant of 90 minutes (the difference from the normal electron density becomes $1/e$ 90 minutes after the launch). Such a flow would be strongly controlled by the local geomagnetic field (inclination ∼43°) because electrons can move only along the field. It would thus influence the lifetime of the hole, i.e. those in equatorial regions may decay faster because electrons can flow horizontally there (i.e. flow from the black part to the white part in Fig. 3(b, d)). Bernhardt *et al*. (2001) reported that the hole made by the OMS burn above Peru recovered within 10 minutes, much faster than the present case.

Papagiannis and Mendillo (1975) suggested the possibility of using the ionospheric hole as a window for low frequency radio waves from space. Bernhardt and da Rosa (1977) proposed to use the thinned ionosphere as a lens to realize a refracting radio telescope. Such ground based low frequency astronomical observations were performed later in the artificial electron depletion experiments to release neutral molecules from the OMS of Space Shuttle. Mendillo *et al*. (1987) successfully took the radio spectrum of emissions from our galaxy in frequencies 1.7–2.7 MHz in Australia through this artificial window. In their experiment, the released gas weighed 244 kg, which corresponds to only ∼1 second burn of the H-IIA first stage engine. H-IIA launches would thus make longer-lasting windows with thinner electron contents. H-IIA launches with similar ascending tracks occur a few times a year, and installation of a simple observatory, e.g. at the Daito Islands (Fig. 1) located just beneath the hole, would offer a cheap opportunity for pilot radio astronomical observations in low frequencies, which is otherwise possible only from space, e.g. using a radio telescope onboard a lunar orbiting satellite (Novaco and Brown, 1978).

References

Afraimovich, E. L., E. A. Kosogorov, and O. S. Lesyuta, Effects of the August 11, 1999, total solar eclipse as deduced from total electron content measurements at the GPS network, *J. Atmos. Solar-Terrestrial Phys.*, **64**, 1933–1941, 2002.

Agnew, D. C. and K. M. Larson, Finding the repeat time of the GPS constellation, *GPS Solutions*, **11**, 71–76, 2007.

Bernhardt, P. A., Three-dimensional, time-dependent modeling of neutral gas diffusion in a nonuniform, chemically reactive atmosphere, *J. Geophys. Res.*, **84**, 793–802, 1979a.

Bernhardt, P. A., High-altitude gas releases: transition from collisionless flow to diffusive flow in a nonuniform atmosphere, *J. Geophys. Res.*, **84**, 4341–4354, 1979b.

Bernhardt, P. and A. V. da Rosa, A refracting radio telescope, *Radio Sci.*, **12**, 327–336, 1977.

Bernhardt, P. A., J. D. Huba, W. E. Swartz, and M. C. Kelley, Incoherent scatter from space shuttle and rocket engine plumes in the ionosphere, *J. Geophys. Res.*, **103**, 2239–2251, 1998.

Bernhardt, P. A., J. D. Huba, E. Kudeki, R. F. Woodman, L. Condori, and F. Villanueva, Lifetime of a depression in the plasma density over Jicamarca produced by space shuttle exhaust in the ionosphere, *Radio Sci.*, **36**, 1209–1220, 2001.

Bernhardt, P. A., P. J. Erickson, F. D. Lind, J. C. Foster, and B. W. Reinisch, Artificial disturbances of the ionosphere over the Millstone Hill Incoherent Scatter Radar from dedicated burns of the space shuttle orbital maneuver subsystem engines, *J. Geophys. Res.*, **110**, doi:10.1029/2004JA010795, 2005.

Booker, H. G., A local reduction of F-region ionization due to missile transit, *J. Geophys. Res.*, **66**, 1073–1079, 1961.

Calais, E. and J. B. Minster, GPS detection of ionospheric perturbations following a Space Shuttle ascent, *Geophys. Res. Lett.*, **23**, 1897–1900, 1996.

Calais, E., J. B. Minster, M. A. Hofton, and H. Hedlin, Ionospheric signature of surface mine blasts from Global Positioning System measurements, *Geophys. J. Int.*, **132**, 191–202, 1998.

Donn, W. L., E. Posmentier, U. Fehr, and N. K. Balachandran, Infrasound at long range from Saturn V, 1967, *Science*, **162**, 1116–1120, 1968.

Mendillo, M., G. S. Hawkins, and J. A. Klobuchar, A sudden vanishing of the ionospheric F region due to the launch of Skylab, *J. Geophys. Res.*, **80**, 2217–2225, 1975.

Mendillo, M., J. Baumgardner, D. P. Allen, J. Foster, J. Holt, G. R. A. Ellis, A. Klekociuk, and G. Reber, Spacelab-2 plasma depletion experiments for ionospheric and radio astronomical studies, *Science*, **238**, 1260–1264, 1987.

Mitchell, C. N., L. Alfonsi, G. De Franceschi, M. Lester, V. Romano, and A. W. Wernik, GPS TEC and scintillation measurements from the polar ionosphere during the October 2003 storm, *Geophys. Res. Lett.*, **32**, doi:10.1029/2004GL021644, 2005.

Novaco, J. C. and L. W. Brown, Nonthermal galactic emission below 10 megahertz, *Astrophys. J.*, **221**, 114–123, 1978.

Osawa, H., *Shinban Nippon Rocket Monogatari (Story about Japanese Rockets, New Edition)*, 277 pp, Seibundo-Shinkosha, Tokyo, 2003 (in Japanese).

Papagiannis, M. D. and M. Mendillo, Low frequency radio astronomy through an artificially created ionospheric window, *Nature*, **255**, 42–43, 1975.

Saito, A., M. Nishimura, M. Yamamoto, S. Fukao, T. Tsugawa, Y. Otsuka, S. Miyazaki, and M. C. Kelley, Observations of traveling ionospheric disturbances and 3-m scale irregularities in the nighttime F-region ionosphere with the MU radar and a GPS network, *Earth Planets Space*, **54**, 31–44, 2002.

Zhang, D. H. and Z. Xiao, Study of ionospheric response to the 4B flare on 28 October 2003 using International GPS Service network data, *J. Geophys. Res.*, **110**, doi:10.1029/2004JA010738, 2005.

T. Furuya and K. Heki (e-mail: heki@mail.sci.hokudai.ac.jp)